Determination of Dendrigraft Poly-L-Lysine Diffusion Coefficients by Taylor Dispersion Analysis

Hervé Cottet,*,† Michel Martin,‡ Alain Papillaud,† Eddy Souaïd,† Hélène Collet,† and Auguste Commeyras†

Institut des Biomolécules Max Mousseron (IBMM, UMR 5247 CNRS-Université de Montpellier 1-Université de Montpellier 2), place Eugène Bataillon CC 017, 34095 Montpellier Cedex 5, France, and Ecole Supérieure de Physique et de Chimie Industrielles, Laboratoire de Physique et Mécanique des Milieux Hétérogènes (PMMH-UMR 7636 CNRS-ESPCI-Université Paris 6-Université Paris 7), 10 rue Vauquelin, 75231 Paris Cedex 05, France

Received March 6, 2007; Revised Manuscript Received May 7, 2007

This work focuses on the physicochemical characterization of dendrigraft poly-L-lysines (DGLs) obtained by polymerization of *N*-carboxyanhydride in buffered water (pH 6.5). Diffusion coefficients (D) and hydrodynamic radii (R_h) of five successive DGL generations were determined by Taylor dispersion analysis (TDA). To our knowledge, this is the first experimental work using TDA for the characterization of dendrimer-like structures. Experimental R_h values obtained by TDA were compared to those derived from dynamic light scattering and size exclusion chromatography coupled to a triple detection (refractive index, viscosimetry, and static light scattering). Significant differences were obtained, especially for the highest generations, as a result of the inherent contribution of aggregates to the light scattering intensity. For that reason, TDA was found to be the most appropriate technique for determining the D values of these hyperbranched macromolecules. Regarding their physicochemical behavior, the experimental results confirm that DGLs are very similar to trifunctional dendrimers (exponential growth of the molar mass, almost linear variation of the hydrodynamic radius, high branching density, and maximum of the intrinsic viscosity or of the free volume fraction for generation 4).

1. Introduction

Several techniques are available for measurement of diffusion coefficients (D), including free diffusion,[1] sedimentation,[2] dynamic light scattering (DLS),[3] pulsed NMR techniques,[4] chromatographic methods such as hydrodynamic chromatography (HDC)[5] or size exclusion chromatography (SEC),[6] capillary electrophoresis,[7−9] and Taylor dispersion (or diffusion) analysis (TDA).[10−13] TDA is an absolute, simple, and rapid method for determining D values. It is based on the dispersion of a solute plug in a solvent flow under a dispersive velocity profile (laminar Poiseuille flow). The band dispersion is directly related to the molecular diffusion that redistributes the molecules over the cross section of the tube.[10] TDA is applicable on (macro)molecules of virtually any molar mass. Despite the advantages of this method, TDA has not been extensively used. There are very few works dealing with the use of TDA for polymer analysis. Boyle et al.[14] used TDA (they named it flow injection analysis) to determine coefficient diffusions of pauci- and polydisperse poly(styrene sulfonate) (PSS) samples. Mes et al.[15] reported a comparison of different methods (DLS, TDA, HDC, and SEC) for the determination of diffusion coefficients of synthetic polymers (styrene acrylonitrile copolymers). They concluded that all these methods can be used to accurately determine diffusion coefficients when the polymer samples have low polydispersities. For polydisperse samples, TDA was described as the method of choice when care is taken to avoid the presence of low-molar-mass UV absorbing impurities.

The dendritic topology has been recognized as the fourth major class of macromolecular architecture.[16−17] The characterization of dendrimers is crucial for their applications (see refs 18 and 19), such as in nanomaterials, diagnostics, drug delivery, biocides, gene transfer, and catalyst supports. The molecular dimension and the conformation in solution are involved in the control of the efficiency for such applications. The hydrodynamic size of dendrimers in solution is generally obtained from intrinsic viscosity[20−21] (assuming that the molar mass is close to the theoretical value), DLS,[22] or other diffusion measurements such as pulsed NMR.[23−24] To our knowledge, there is no report on the use of TDA for characterizing dendrimers, hyperbranched polymers, or dendritic structures.

Dendrigraft polymers are the most recently discovered subset of dendritic polymers. They are usually synthesized by "protect/deprotect" or activation schemes. Compared to dendrimers, dendrigraft polymers are less controlled. However, the molar mass increases more rapidly with generation than for dendrimers. This dramatic increase in the molar mass combined with the possibility of using relatively inexpensive monomers offers the potential to manufacture and develop dendrigraft polymers possessing dendrimer-like properties at a much lower cost.[25] Klok et al.[26−27] reported the synthesis of dendrigraft (or hyperbranched) poly-L-lysines (DGLs) by polymerization of *N*-carboxyanhydride (NCA) in dimethylformamide. These DGLs were characterized by proton NMR and SEC relative to poly(ethylene oxide).[26] Recently, our group described a new synthetic route to DGLs by polymerization of NCA in water.[28]

The main purpose of this work was to determine the diffusion coefficients (and hydrodynamic radii) of five generations of DGLs by TDA. A second objective was to compare the values

* Corresponding author: Tel: +33 4 6714 3427. Fax: +33 4 6763 1046. E-mail: hcottet@univ-montp2.fr.
† Institut des Biomolécules Max Mousseron.
‡ Ecole Supérieure de Physique et de Chimie Industrielles.

10.1021/bm070268j CCC: $37.00
Published on Web 09/06/2007

obtained by TDA to those derived from DLS and from SEC coupled to a triple detection.

2. Theoretical Background

TDA is based on the dispersion of a solute plug in a laminar Poiseuille flow.[10,11] In a cylindrical capillary tube, the velocity profile is a parabolic function of the radius, reaching its maximum at the capillary axis and with zero value at the capillary wall. Molecules injected in a narrow band at the inlet end of the capillary tube move with different velocities depending to their positions in the capillary cross section. Molecular diffusion redistributes the molecules over both the cross section and the tube axis. The combination of the dispersive velocity profile with the molecular diffusion leads to a specific mechanism of dispersion described by the Taylor−Aris−Golay equation for unretained solutes:[10−12]

$$H = \frac{2D}{u} + \frac{{d_c}^2 u}{96D} \tag{1}$$

where H is the height of an equivalent theoretical plate, u is the average velocity of the mobile phase, d_c is the capillary diameter, and D is the molecular diffusion coefficient. The plate height, H, of a peak is related to the two first moments of the elution profile by

$$H = \frac{l_d m_2}{{m_1}^2} \tag{2}$$

where m_1 is the first moment of the distribution (average elution time), and m_2 is the second moment of the distribution (temporal variance of the elution peak). The term l_d is the capillary length to the detector. Mathematically, m_1 and m_2 can be determined by integration of the elution profile according to eqs 3 and 4:

$$m_1 = \frac{\int h(t) t \mathrm{d}t}{\int h(t) \mathrm{d}t} \tag{3}$$

$$m_2 = \frac{\int h(t)(t - m_1)^2 \mathrm{d}t}{\int h(t) \mathrm{d}t} \tag{4}$$

where $h(t)$ is the detector response. Equation 1 can be rewritten as a function of the applied pressure P:

$$H = \frac{64\eta L D}{{d_c}^2} \times \frac{1}{P} + \frac{{d_c}^4}{3072\eta L D} \times P \tag{5}$$

where L is the total capillary length, and η is the mobile phase viscosity. The condition for eqs 1 and 5 to hold true is that the residence time t of the solute before detection is much longer than the characteristic diffusion time t_D of the solute in the cross section of the capillary:

$$t \gg \frac{{R_c}^2}{2D} \tag{6}$$

with R_c being the internal radius of the capillary tube. Furthermore, in using eqs 1−5, it is assumed that there is no interaction of the solute with the capillary wall and that the contributions of the sample volume to the two first moments of the elution time distribution are negligible or have been appropriately taken into account.

Three different methodologies were used for performing TDA, i.e., to obtain the diffusion coefficient from the distribution of the elution times recorded by the detector. For short, in the following, they are called the "half-height method", the "linear method", and the "integral method".

In the half-height method, m_1 is measured as the elution time of the peak apex, and m_2 is obtained from the measured peak width at half-height, $w_{1/2}$, as $m_2 = {w_{1/2}}^2/5.54$. This amounts to assimilating the peak shape to a Gaussian curve. The diffusion coefficient is related to H by assuming that the measurement is made at a velocity large enough for the first term of eq 1 to be negligible:

$$D = \frac{{d_c}^2 u}{96H} = \frac{{d_c}^4 P}{3072\eta L H} \tag{7}$$

The D values reported for this method are averages from several repetitions of the TDA at a given mobilizing pressure.

In the linear method, experiments were performed at various carrier velocities. For each velocity, H was calculated from eq 2 using m_1 and m_2 values obtained, as above, from the elution time at the peak apex and the peak width at half-height, respectively. Then D was determined from the slope, S, of the ascending branch of the H versus u plot as

$$D = \frac{{d_c}^2}{96S} \tag{8}$$

This method allows one to get rid of the flow-independent potential contribution to m_2, and thus improves the accuracy.

In the integral method, m_1 and m_2 are obtained from the elution profile by means of eqs 3 and 4, which do not require any hypothesis about the shape of the elution peak. Then D is obtained from the full expression of H (eq 1) as

$$D = \frac{u}{4}\left(H - \sqrt{H^2 - \frac{{d_c}^2}{12}}\right) = \frac{{d_c}^2 P}{128\eta L}\left(H - \sqrt{H^2 - \frac{{d_c}^2}{12}}\right) \tag{9}$$

which applies at any flow velocity. In this method too, the accuracy of D is improved by performing several injections and taking the average of the individual D values.

Finally, the hydrodynamic radii (R_h) of the solutes are calculated using the Stokes−Einstein relationship:

$$D = \frac{kT}{6\pi\eta R_h} \tag{10}$$

where k is the Boltzmann constant.

3. Materials and Methods

3.1. Reagents. Borax (disodium tetraborate decahydrate) was purchased from Prolabo (Paris, France). Mesityl oxide, acetonitrile, phthalic acid, sodium dihydrogenophosphate, disodium hydrogenophosphate, and poly(diallyldimethylammonium chloride) (PDADMAC, M_w 400−500 × 10^3 g/mol) were obtained from Aldrich (Milwaukee, WI). Sodium hydroxide (NaOH) was from Merck (Darmstadt, Germany). The water used to prepare all buffers was further purified with a Milli-Q system from Millipore (Molsheim, France). The borate buffers were directly prepared by dissolving the appropriate amount of borax in water.

A standard of PSS (weight average molecular mass M_w 1.45 × 10^5 g/mol) was purchased from Polymer Standards Service (Mainz, Germany). The polydispersity index of the PSS was below 1.2. The degree of sulfonation of the PSS was higher than 90%.

Scheme 1. Schematic Representation of DGLs from the First Generation (P_1) to the Fifth Generation (P_5)[a]

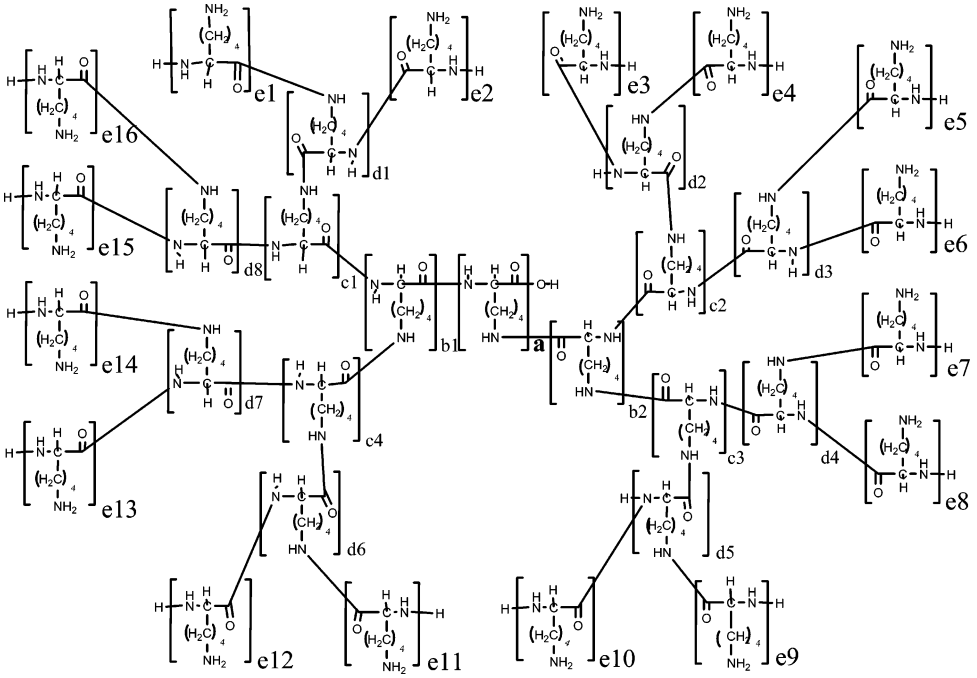

[a] Chemical structures of the DGLs: P_1 ($N = 8$, $a = 8$); P_2 ($N = 48$, structure of P_1 and $\sum_{i=1}^{2} b_i = 40$); P_3 ($N = 123$, structure of P_2 and $\sum_{i=1}^{4} c_i = 75$); P_4 ($N = 365$, structure of P_3 and $\sum_{i=1}^{8} d_i = 342$); P_5 ($N = 963$, structure of P_4 and $\sum_{i=1}^{16} e_i = 598$). N is the total average degree of polymerization. The terms a, b_i, c_i, d_i, and e_i correspond to the average degree of polymerization within a branch of the molecule. All these average values were obtained using the DGL average molar masses determined by SEC (see Table 1).

3.2. Buffers. Three different buffers were used in this study. Buffer 1 was prepared by dissolving 50 g/L $H_2PO_4^-$, Na^+ in water (pH 4.5, 0.61 M ionic strength, 1.01 10^{-3} Pa·s viscosity at 25 °C). Buffer 2 was made of 48.5 g/L $H_2PO_4^-$, Na^+ in water/acetonitrile (97/3) v/v (pH ∼ 4.5, 0.59 M ionic strength, 1.08 10^{-3} Pa·s viscosity at 25 °C). Buffer 3 was prepared by dissolving 38 mM NaH_2PO_4, 38 mM Na_2HPO_4, and 154 mM NaCl (pH adjusted to 7.0, 0.306 M ionic strength, 0.91 10^{-3} Pa·s viscosity at 25 °C).

3.3. Dendrigraft Poly-l-lysines. Five generations of DGLs, noted P_1-P_5, were synthesized according to a recently described protocol.[28] Briefly, the DGLs were synthesized by ring-opening polymerization of NCAs of N_ϵ-trifluoroacetyl-L-lysine (TFA-L-lysine) using a succession of polymerization and deprotection steps. The polymerization step, performed in aqueous carbonate buffer (pH 6.5), leads to poly(N_ϵ-TFA-L-lysine) that precipitates above a certain molar mass. TFA-L-lysine and soluble low molar mass oligomers were eliminated by filtration and by washing the precipitates with water. Next, in the deprotection step, the polymer is unprotected in the N_ϵ position by adding NH_3 in a methanol/water mixture at 40 °C. The unprotected polymer was further freeze-dried and used afterward as a precursor for the synthesis of the next generation. The number average molar mass, the average degree of polymerization (N) and the polydispersity indexes of the five DGL generations were determined in a previous work by SEC coupled with static multi-angle light scattering and refractive index detection[28] (experimental results are reported in Table 1). With this double detection, absolute molar masses are obtained, and there is no need to use standards for the calibration of the column. Polydispersity indexes of DGLs were between 1.20 and 1.46, and the number average molar masses were between 1400 (P_1) and 169000 g/mol (P_5). For a better understanding and visualization of the DGL chemical structures, the reader can refer to Scheme 1.

3.4. Taylor Dispersion Analysis. TDA experiments were performed on a PACE MDQ Beckman Coulter (Fullerton, CA) apparatus. Capillaries were prepared from bare silica tubing purchased from Composite Metal Services (Worcester, United Kingdom). Capillary dimensions were 60 cm (50 cm to the detector) × 50 μm i.d. New capillaries were conditioned with the following flushes: 1 M NaOH for 30 min, 0.1 M NaOH for 30 min, and water for 10 min. Before sample injection, the capillary was filled with the selected buffer. Samples were dissolved in buffer at 2−8 g/L, filtered with a 0.45 μm filter, and introduced hydrodynamically on the inlet side of the capillary (0.4 psi, 9s). Different mobilization pressures were applied (between 0.1 and 10 psi) with buffer vials at both ends of the capillary. The mobilization pressure value is specified on the figures and tables (0.2 psi for DGL analysis). Solutes were monitored by UV absorbance at 200 nm. The temperature of the capillary cartridge was set at 25 °C.

Table 1. Average Molar Masses (M_n), Average Degrees of Polymerization (N), and Polydispersity Indexes (I) of Five DGL Generations (P1 to P5)[a]

	P_1	P_2	P_3	P_4	P_5
M_n (g/mol)[b]	1450	8600	22000	65300	172300
N	8	48	123	365	963
I	1.20	1.38	1.46	1.36	1.46

[a] These physicochemical parameters were obtained by SEC coupled to static light scattering and refractive index detection for P_2-P_5, and by capillary electrophoresis for P_1.[28] [b] Degrees of polymerization were calculated by assuming that the average molar mass of a monomer is 179 g/mol. This average molar mass of the monomer was obtained on the basis that 51% of the monomers were condensed by phosphate counterions in the eluent (Manning's condensation theory[37]).

For TDA of phthalate and PSS, the capillary was successively flushed, between two TDA analyses, with: (i) water (50 psi, 1 min); (ii) 1 M NaOH (50 psi, 2 min), and (iii) buffer (50 psi, 3 min).

For TDA of DGLs, the fused silica capillary was initially noncovalently coated with a polycation (PDADMAC) in order to prevent solute adsorption onto the capillary wall. The coating was performed by flushing the capillary with (i) 0.2% PDADMAC containing 2 M NaCl in water (50 psi, 15 min) and (ii) pure water (50 psi, 5 min). Between two TDA analyses, the capillary was successively flushed with (i) water (50 psi, 1 min) and (ii) buffer (50 psi, 1.5 min). A 2 M NaCl solution was used in the PDADMAC coating solution to increase the thickness of the PDADMAC layer deposited on the capillary surface.

3.5. SEC Coupled to a Triple Detection. SEC was performed on a Viscotek chromatograph (GPCmax, Houston, TX) using a Triple Detector Array 302 (Viscotek, Houston, TX) with refractive index,

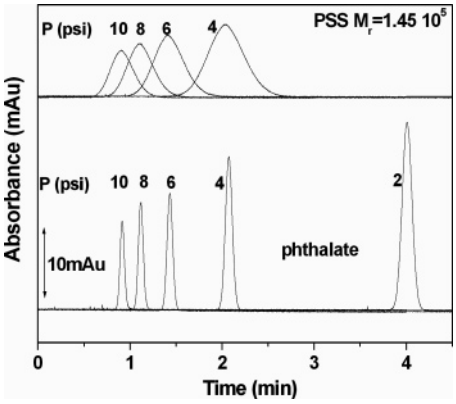

Figure 1. Overlay of the TDA signals obtained for phthalate and a standard of PSS ($M_r = 1.45 \times 10^5$) at different mobilization pressures. Fused silica capillary, 60 cm (50 cm to the detector) × 50 μm i.d. All experiments were performed in 80 mM borate buffer, pH 9.2. Samples at 0.5 g/L in buffer. Hydrodynamic injection: 0.4 psi, 9s. UV detection at 200 nm. Temperature: 25 °C.

viscosity, and static light scattering (at 7° and 90° angles). The mobile phase was buffer 2 (see section 3.2). The flow rate was 0.6 mL/min. Samples were prepared at 3−5 g/L in the eluent and stirred for 5 h. Sample solutions were next filtered with a 0.45 μm Nylon filter, injected through a 100 μL loop, and eluted in a Superose 12 HR 10/30 column. The temperature was set at 28 °C. The detector alignment and instrument sensitivity parameters were previously calibrated using a pullulan standard. Within 10% variations, the d*n*/d*c* values were equal to 0.185 for all the DGL samples. This value is in agreement with typical d*n*/d*c* value obtained for proteins such as bovine serum albumin.[29]

3.6. Dynamic Light Scattering. DLS experiments were performed on a Zetasizer Nano ZS apparatus (Malvern Instruments, Worcestershire, U.K.). The detector position was at 173° from the laser incidence (close to backscatter detection). Samples were prepared at 2−8 g/L in the buffer and filtered with a 0.45 μm filter. DLS measurements were performed at 25 °C in disposable polystyrene cuvettes (750 μL).

4. Results and Discussion

4.1. TDA of Well-Characterized Molecule and Polyelectrolyte. Before applying the TDA to the five generations of DGLs, we first determined the diffusion coefficients of a well-characterized molecule and polyelectrolyte. For that, we used phthalate and a standard of PSS ($M_w = 1.45 \times 10^5$ g/mol) as model compounds. The TDA was performed using a 80 mM borate buffer (pH 9.2) as the mobile phase and a 60 cm-long fused silica capillary (50 cm to the detector) with an internal diameter of 50 μm. Figure 1 shows the UV traces obtained for both compounds at different mobilization pressures (between 2 and 10 psi). Since the two compounds were not retained in the capillary column, the detection times are the same for the two (macro)molecules. For both solutes, the maximum absorbance of the peak decreases with increasing mobilizing pressure because of higher dispersion. At a given mobilizing pressure, the peak widths are much higher for PSS than for phthalate because of the difference in the diffusion coefficients. Both effects reflect the fact that, for all selected mobilizing pressures, the plate height is dominantly controlled by the second term of eq 1. It is worth noting that eq 6 was verified since the detection time (between 1 and 4 min, see Figure 1) was much higher than the characteristic diffusion time t_D (0.5 s for phthalate and 14 s for PSS $M_r = 1.45 \times 10^5$).

By applying the *half-height method* (see section 2), diffusion coefficients were determined for each mobilization pressure by measuring the peak width. The corresponding D values are plotted in Figure 2A,B. The second method (*linear method*) is based on the linear dependence given by eq 5 and consists of plotting the H values as a function of the mobilization pressure (see Figure 2A,B). The slope of the plot ($d_c^4/3072\eta LD$) is directly related to the diffusion coefficient. In the experimental conditions used in this work, eq 7 is valid, and H values increase linearly with the applied pressure as demonstrated for both solutes by Figure 2A,B. From Figure 2, the extrapolation of the H value at zero pressure also demonstrates that the contribution to the peak dispersion due to the injection (which is an additional contribution to H, independent of the pressure) is negligible (injection volume ~ 7 nL). The third method for determining D values (*integral method*) is based on the integration of the whole UV trace (see section 2). Table 2 gathers the diffusion coefficient values obtained for both solutes using the three aforementioned methods. At the level of 0.05, the results obtained by the three data processing methods are not significantly different. The experimental D values are in good agreement with literature data derived from ionic limiting mobility (phthalate) or from viscosity data at similar ionic strength (PSS).

To confirm that, under our conditions, external contributions to the peak dispersion remain negligible, the corrections for the finite width of the injected plug on the average retention time (m_1) and on the observed temporal variance (m_2) were evaluated according to the following equations (see appendix):

$$m_{1,\mathrm{corr}} = \frac{m_1}{1 - \dfrac{V_i}{2V_c}} \tag{11}$$

$$m_{2,\mathrm{corr}} = \frac{1}{1 - \dfrac{V_i}{V_c}}\left[m_2 - \frac{m_1^2}{12}\frac{\left(\dfrac{V_i}{V_c}\right)^2}{\left(1 - \dfrac{V_i}{2V_c}\right)^2}\right] \tag{12}$$

where V_i is the injected volume (~7 nL in our conditions), and V_c is the capillary volume from inlet to detector, equal to $\pi d_c^2 l_d/4$. Correction on the elution time (m_1) is below 0.4% independently of the solute and the mobilizing pressure. Correction on the temporal variance (m_2) was always lower than 0.9% as calculated using eq 12. In a recent work,[30] Sharma et al. also pointed out the possible influence of the pressure ramp on the determination of D. They demonstrated that significant error could arise, especially for low elution times (high pressure and/or short capillary lengths). In our conditions, the correction on elution times due to the pressure ramp remains limited (0.9% at 3 psi and 4.5% at 10 psi). This was confirmed by the experimental linear behavior of H as function of P obtained in Figure 2 (at higher pressure, deviation from linearity is expected).

On the whole, the three methods are in very good agreement with each other (differences between methods lower than 2%). However, the integral method appeared to be the method of choice because of the lower dispersion of the D values (see relative standard deviations (RSDs) in Table 2).

4.2. TDA of DGLs. In a second series of experiments, we performed TDA on the five successive generations of DGL. Scheme 1 depicts the general hyperbranched (or dendrigraft) chemical structure of DGL. To avoid any adsorption of the cationic DGLs onto the capillary wall, the fused silica capillary was beforehand coated by flushing the capillary with an aqueous solution of a polycation (PDADMAC, see experimental section

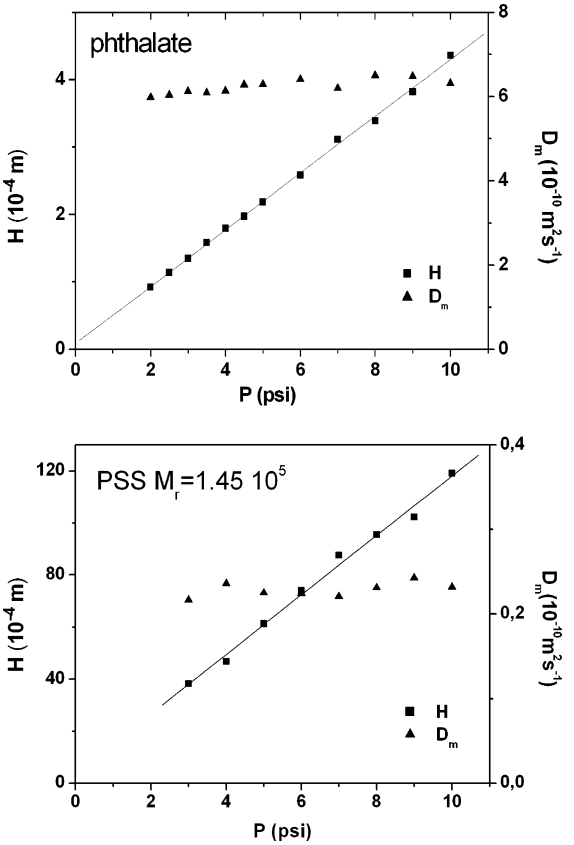

Figure 2. Variation of the heights equivalent to a theoretical plate (*H*, scale on the left) and of the diffusion coefficient (D_m, scale on the right) as a function of the mobilizing pressure. Same experimental conditions as Figure 1.

Table 2. Influence of the Calculation Method on the Determination of the Diffusion Coefficients of Two Model Compounds (Phthalate and PSS Standard)[a]

	phthalate		PSS $M_r = 1.45 \times 10^5$	
method	$\langle D \rangle^b$	RSD[b](%)	$\langle D \rangle^c$	RSD[c](%)
half-height	6.33×10^{-10}	7.4	2.28×10^{-11}	3.7
linear	6.34×10^{-10}		2.31×10^{-11}	
integral	6.42×10^{-10}	2.6	2.32×10^{-11}	2.3
literature values	6.8×10^{-10} [d]		2.1×10^{-11} [e]	

[a] Experimental conditions as in Figure 1. [b] Average value for 15 different mobilization pressures between 1 and 20 psi. [c] Average number for eight different pressure values between 3 and 10 psi. [d] Value derived from the ionic mobility of phthalate at infinite dilution in water[38] ($\mu^{0,\infty} = 52.9 \times 10^{-9}$ m^2 V^{-1} s^{-1}) using the following equation: $D = (kT/2e)\mu^{0,\infty}$. [e] Value calculated according to the following equation: $D = (kT/6\pi\eta)(10\pi N_A/3[\eta]M)^{1/3}$, where N_A is the Avogadro constant. Intrinsic viscosity data for PSS in water at 0.05 M ionic strength ($[\eta] = 1.39 \times 10^{-4}$ M$^{0.72}$, $[\eta]$ in dL/g) was taken from ref 39.

for more details). The TDAs were performed using a buffer that was previously used for molar mass determination[28] (buffer 1, a 50 g/L phosphate buffer (pH 4.5)). In this buffer, DGLs are fully protonated. Different mobilizing pressures were applied; however, the best experimental results in terms of peak shape were obtained by using relatively low mobilizing pressure (0.2 psi). The five UV traces corresponding to the TDAs of the five DGL generations are presented in Figure 3. Detection times (about 45 min) were much higher than in Figure 1 (less than 5 min); however, the experimental protocol remained very simple, and the Gaussian shape of the peaks was preserved. Distortion of the Gaussian peak shape was observed for pressures higher than 0.4 psi. The exact cause of this distortion is not known.

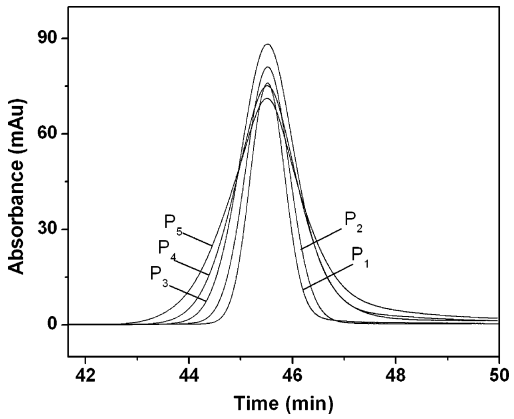

Figure 3. TDA (UV traces) of the five DGL generations. PDADMAC-coated capillary, 60 cm (50 cm to the detector) × 50 μm i.d. Mobilization pressure: 0.2 psi. Experiments were performed in buffer 2 (see section 3.2). Samples at 8 g/L in buffer 2. Hydrodynamic injection: 0.4 psi, 9s. Other conditions as in Figure 1.

The condition expressed by relation 6 for eq 1 to be valid is well satisfied. A possibility exists that the distortion arises from the viscosity difference between the sample and the carrier liquid, although it is moderate (not exceeding 30%). As expected from eq 5, the higher the generation, the higher the hydrodynamic radius, the lower the diffusion coefficient, and the higher the peak dispersion is. Indeed, the second term proportional to *P* in eq 5 becomes preponderant when the mobilizing pressure exceeds 0.065 psi for P_1 and 0.011 psi for P_5. In these experimental conditions, diffusion coefficients of the five DGL generations were determined by using the integral method. The condition of eq 6 was verified since the DGL characteristic diffusion times were below 10 s, while the detection time was about 2750 s (see Figure 3). Because of relatively high elution times, corrections due the finite width of the injected plug on the average retention time (see eq 11) and due to the initial pressure ramp[30] are both very low (<0.4%). In the first approximation, corrections due to the finite width of the injected plug on temporal peak variance (eq 12) were not considered since they were evaluated below 4.8% for P_2-P_5 and below 9.4% for P_1. Since we were interested in the macromolecule dimensions, the results were presented in terms of hydrodynamic radius (see Table 3). The RSDs on R_h values, calculated on five successive experiments, were below 5%. It is worth noting that the concentration of the DGL sample (from 2 to 8 g/L) did not significantly change the diffusion coefficient values within ~10% variations (not shown). This was expected since the DGL-injected concentrations are much lower than the overlap concentrations (estimated from 250 to 550 g/L, depending on the generation), and since the cross-sectional average concentration of the sample zone is everywhere lower than the injected concentration as the zone migrates along the capillary.

4.2.1. Influence of the Buffer Composition. Diffusion coefficients were next determined in two other buffers (see section 3.2 for exact compositions and Table 3 for R_h values). Except for the first generation (P_1) in buffer 3, the RSDs calculated on five successive experiments were always below 5%. As demonstrated by Figure 4, the hydrodynamic radii of the DGLs increase almost linearly with the number of generations (at least up to generation 4). This is reminiscent of the behavior of dendrimers.[31] Deviation from linearity for higher generations (P_5) could be due to the influence of aggregates on the measurement of the unimer dimension (see discussion below). For all the DGLs, R_h was found to decrease after the addition of organic solvent (3% acetonitrile in volume, see buffer 2 vs

Table 3. Hydrodynamic Radii and Intrinsic Viscosities of Five DGL Generations (P_1 to P_5)[a]

		P_1	P_2	P_3	P_4	P_5
buffer 1	R_h (nm) TDA[b]	1.03 (3%)	1.96 (1%)	3.06 (2%)	3.69 (5%)	6.39 (2%)
	R_h (nm) DLS[c]	1.12 (17%)	2.21 (9%)	3.23 (8%)	5.98 (8%)	7.94 (8%)
buffer 2	R_h (nm) TDA[b]	0.84 (2%)	1.6 (1%)	2.33 (1%)	3.48 (3%)	4.52 (1%)
	R_h (nm) DLS[c]	0.97 (26%)	1.94 (8%)	3.28 (12%)	5.27 (6%)	7.49 (13%)
	R_h (nm) SEC[d(1)]		1.79	2.95	4.95	7.4
	R_h (nm) SEC[d(2)]		1.66	2.51	4.12	5.62
	$[\eta]$ (mL/g)[d]		5.6	6.6	7.1	6.4
buffer 3	R_h (nm) TDA[b]	0.77 (11%)	1.4 (5%)	2.14 (1%)	3.00 (2%)	4.43 (1%)
	R_h (nm) DLS[c]	1.05 (ND)	1.77 (ND)	3.43 (13%)	6.15 (15%)	7.16 (17%)

[a] Hydrodynamic radii were calculated from the diffusion coefficients determined by TDA, DLS, or SEC coupled to a triple detection using eq 10. The buffer viscosities are given in section 3.2. for TDA and DLS, and the RSDs are given in percentages ($n = 5$ experiments). [b] Experimental conditions as in Figure 3 in the mentioned buffer. [c] See Material and Methods section for experimental conditions. [d] Hydrodynamic radius and intrinsic viscosity were determined by SEC coupled to a triple detection. See Material and Methods section for experimental conditions. (1) Values obtained by integration of the whole unimer peak. (2) Values obtained at the apex of the unimer peak.

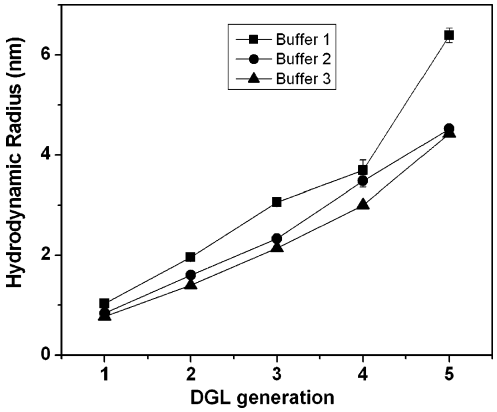

Figure 4. Variation of the DGL hydrodynamic radius determined by TDA as a function of the generation in three different buffers. Experiments were performed in the mentioned buffer (see section 3.2). Samples at 8 g/L in the mentioned buffer. Other experimental conditions as in Figure 3.

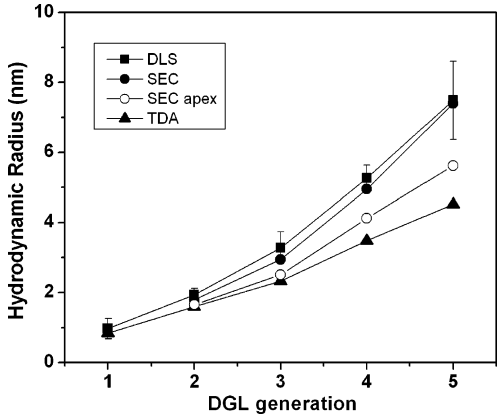

Figure 5. Comparison of the hydrodynamic radius values obtained by DLS, SEC with triple detection, and TDA methodologies for five DGL generations. Experimental conditions as in Figure 3 for the TDA analysis. See experimental section for the DLS and SEC experimental conditions.

buffer 1 compositions). This can be explained by a decrease in the solvent quality with the addition of organic modifier. In neutral pH conditions (buffer 3, pH 7.0), the DGL radii were significantly lower than those at pH 4.5 for comparable ionic strength conditions (buffer 1). These results are in agreement with a decrease in the DGL protonation that diminishes the electrostatic repulsion between amine groups and, as a consequence, reduces the hydrodynamic radii. The pH effect should even be more pronounced at lower ionic strength and/or at pH values higher than 7.

4.2.2. Comparison between TDA, DLS, and SEC Coupled to a Triple Detection. Finally, hydrodynamic radii obtained by TDA were compared with those derived from DLS and SEC coupled to a triple detection (refractive index, viscosity, and static light scattering). All the experimental values are gathered in Table 3. Figure 5 allows the comparison between the three techniques for the determination of DGL hydrodynamic radii in buffer 2. It clearly shows that DLS and SEC coupled to triple detection led to higher values than did TDA. Higher discrepancies were obtained for higher generations (up to 65%). These differences were explained by the existence of DGL aggregates in the sample solutions. The presence of aggregates was established by the bimodal size distribution obtained by DLS. The first mode at low R_h values (between 1 and 10 nm, depending on the generation) was due to DGL unimers, while the second mode (between 50 and 200 nm) was assigned to DGL aggregates. These aggregates could result from hydrogen bonding between unimers. Despite the low proportion of aggregates in mass concentration, the contribution to the light

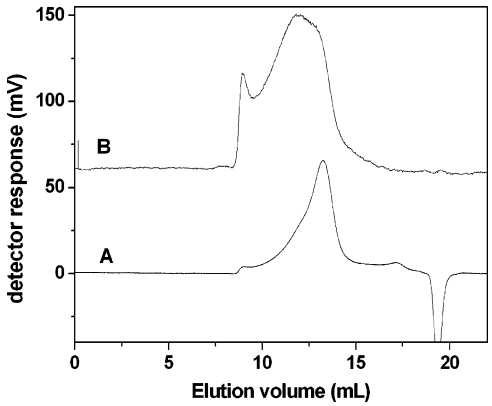

Figure 6. Refractive index (A) and low angle light scattering (B) traces of the SEC chromatogram obtained for P_4 in buffer 2. See Materials and Methods section for experimental conditions.

scattering signal was very important because of the R^6 dependence of the light scattering intensity on the size of the solute.[32] Similarly, in SEC coupled to the triple detection, the refractive index trace displayed a small peak in front of the unimer peak, as exemplified by Figure 6. This figure also clearly demonstrates that very high intensity in the light scattering was obtained at lower elution times (aggregates). R_h values obtained by SEC (integration of the whole unimer peak) were somewhat smaller than those obtained by DLS. A better agreement between TDA and SEC was found when the R_h was taken at the unimer peak apex (see Table 3 and open circles in Figure 5). This can be

explained by the partial separation of the aggregates from the unimers in the column that obviously led to a lesser influence of the aggregates in the light scattering intensity of the unimer peak. However, in the condition of buffer 2, the separation between the unimers and the aggregates is far to be complete (see the shoulder on the unimer peak in Figure 6), indicating that the aggregates still influenced the results obtained for the unimers (main peak).

To gain better insight in the comparison between DLS and TDA measurements, simple calculations based on the theoretical average molecular diffusion coefficients that are measured by each method were performed. Basically, DLS measurement leads to the *z*-average diffusion coefficient[15] as given by eq 13a:

$$\langle D\rangle_{\mathrm{DLS}} = \langle D\rangle_z = \frac{\sum_i N_i M_i^2 D_i}{\sum_i N_i M_i^2} \tag{13a}$$

where N_i is the number of molecules having a molar mass M_i and a diffusion coefficient D_i. The corresponding average hydrodynamic radius is then expressed as

$$\langle R_{\mathrm{h}}\rangle_{\mathrm{DLS}} = \frac{\sum_i N_i M_i^2}{\sum_i \frac{N_i M_i^2}{R_{\mathrm{h},i}}} \tag{13b}$$

Recently, we demonstrated (to be published[33]) that, for TDA, and in the case of a mass concentration sensitive detector, the average diffusion coefficient (or hydrodynamic radius) is given by the following equation:

$$\langle D\rangle_{\mathrm{TDA}} = \frac{\sum_i N_i M_i}{\sum_i \frac{N_i M_i}{D_i}} \tag{14a}$$

$$\langle R_{\mathrm{h}}\rangle_{\mathrm{TDA}} = \frac{\sum_i N_i M_i R_{\mathrm{h},i}}{\sum_i N_i M_i} \tag{14b}$$

Applying these two equations to a bimodal mixture containing P_5 unimer ($R_{\mathrm{h,unimer}} = 4.52$ nm) and different mass proportion of P_5 aggregates (with the assumption that $R_{\mathrm{h,aggregate}} = 10 \times R_{\mathrm{h,unimer}}$ and that $M \sim R_{\mathrm{h}}^{2.8}$ (see section 4.3)) demonstrates that, even at low mass proportion, the influence of aggregates on the average *D* values is highly significant (see Figure 7A for $\langle D\rangle$ values and Figure 7B for the corresponding $\langle R_{\mathrm{h}}\rangle$ values). From Figure 7, it appears that the experimental value of the $\langle R_{\mathrm{h}}\rangle_{\mathrm{DLS}}/\langle R_{\mathrm{h}}\rangle_{\mathrm{TDA}}$ ratio (1.65 for buffer 2, see Table 3) would be observed for a concentration as low as 0.16% (w/w) of aggregates, leading then to $\langle R_{\mathrm{h}}\rangle_{\mathrm{TDA}} = 4.58$ nm and $\langle R_{\mathrm{h}}\rangle_{\mathrm{DLS}} = 7.54$ nm, very close to the experimental $\langle R_{\mathrm{h}}\rangle_{\mathrm{DLS}}$ and $\langle R_{\mathrm{h}}\rangle_{\mathrm{TDA}}$ values. If the size of the aggregates was only 5 times larger than that of the unimers, the same $\langle R_{\mathrm{h}}\rangle_{\mathrm{DLS}}/\langle R_{\mathrm{h}}\rangle_{\mathrm{TDA}}$ ratio would be observed for a 1.5% (w/w) concentration of aggregates. As demonstrated by eq 14b, $\langle R_{\mathrm{h}}\rangle_{\mathrm{TDA}}$ corresponds to the weight average hydrodynamic value. Therefore, TDA is less sensitive to the aggregates than DLS since the contribution of the aggregates to the detector signal is proportional to the mass concentration of aggregates and not to R^6 as for light scattering.

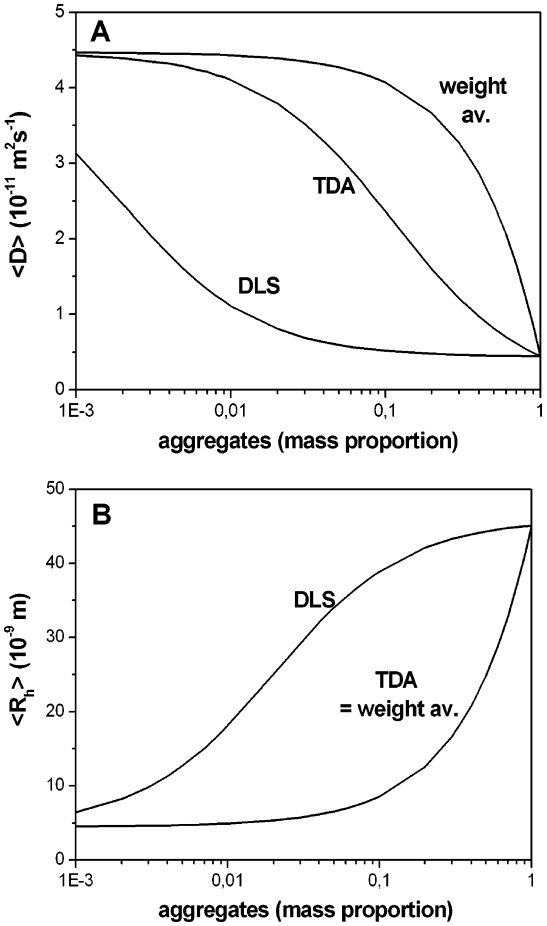

Figure 7. Comparison between calculated average diffusion coefficients (A) and the corresponding hydrodynamic radii (B) obtained by DLS and by TDA as a function of the mass proportion of aggregates for a bimodal mixture containing P_5 unimers and aggregates. For comparison, the weight average values are also plotted on the graphs (note that $\langle R_{\mathrm{h}}\rangle_{\mathrm{TDA}} = \langle R_{\mathrm{h}}\rangle_{\mathrm{W}}$). Calculations were performed according to eqs 15 and 16. Calculations were based on $R_{\mathrm{h,unimer}} = 4.52$ nm, $R_{\mathrm{h,aggregate}} = 10 \times R_{\mathrm{h,unimer}}$, and assuming that $M \sim R_{\mathrm{h}}^{2.8}$ (see section 4.3).

As shown in Table 3, differences in the R_{h} values between DLS and TDA were more marked in buffers 2 and 3. As discussed in section 4.2.1., the addition of organic solvent or the increase in the pH seems to decrease the solvent quality and could thus facilitate the formation of aggregates. For that reason, buffer 1 was considered the best eluent for limiting aggregates and should thus be preferred for the molar mass characterization of DGLs.[28]

4.3. Physicochemical Characteristics of DGLs. The physicochemical characteristics of DGLs are relatively close to a classical dendritic behavior. First, the molar mass of DGLs is an exponential function of the number of generations.[28] More precisely, DGL molar mass between two generations is multiplied by a factor of 3.2[28] (instead of 2 for trifunctional dendrimers such as polylysine dendrimers). Second, as discussed in section 4.2.1, the DGL hydrodynamic radius increases almost linearly with the generation, as for dendrimers. Figure 8 gives other support to the dendritic behavior of DGL by plotting the hydrodynamic radius as a function of the molar mass using a double logarithm scale. Scaling exponents ν in the following equation $R_{\mathrm{h}} \sim M^{1/\nu}$ were derived from linear fits (solid lines in

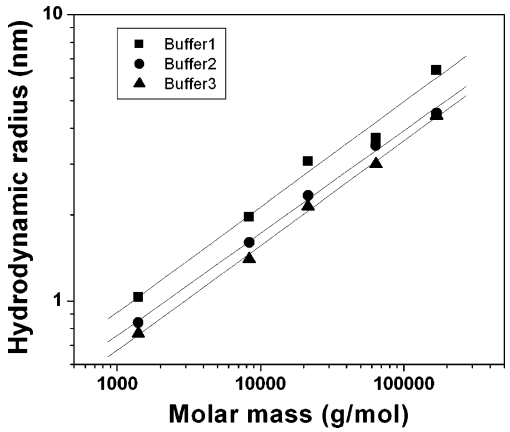

Figure 8. Hydrodynamic radius of DGL as a function of molar mass in double logarithm scale. Solid lines are linear fits with scaling exponents 0.37 ± 0.03 (buffer 1); 0.36 ± 0.01 (buffer 2); and 0.37 ± 0.01 (buffer 3). See section 3.2 for the buffer composition.

Table 4. Hydrodynamic Volumes ($4\pi R_h^3/3$), van der Waals Volumes (V_W), and Free Volume Fractions (f) of DGLs in Buffer 2

DGL	V_h (nm^3)	V_W (nm^3)	f
1	4.58	0.99	0.60
2	31.5	5.9	0.66
3	120	15.1	0.72
4	210	44.8	0.75
5	1093	118	0.69

[a] V_w and f values were obtained using eqs 17 and 18. See the text for more details.

Figure 8). This exponent was assumed to be an indicator of the dendrimer branching behavior.[34] A scaling exponent greater than 3 exceeds the spatial dimensions available, which means that the growth of the molecule cannot continue at all branches. For the three buffers, a scaling exponent ν of 2.8 has been found, in good accordance with typical values obtained for trifunctional dendrimers (poly(ether amide)[34] and poly(propylene imine)[35]). This result is also in good accordance with the high branching ratios of DGLs derived from proton NMR measurements.[28] The branching ratio is defined as the ratio of the number N_ϵ of amine groups that reacted from generation P_n to generation P_{n+1} divided by the total number of N_ϵ amine groups of generation P_n. Branching ratio values between 65% for P_4-P_5 and 100% for P_1-P_2 were determined as compared to a maximal 30% value for the polylysines synthesized by Klok et al.[26] Finally, as demonstrated by Table 3, the intrinsic viscosity (a physicochemical parameter inversely proportional to the macromolecule density in solution) reaches a maximum for the fourth generation, exactly as that for trifunctional dendrimers. If absolute values of intrinsic viscosity should be considered with caution because of the possible influence of aggregates, the position of the maximum is informative. Very similar results were obtained on free volume fractions f calculated according to eq 17:

$$f = 1 - \frac{V_W}{V_h} \tag{17}$$

where V_w is the van der Waals volume, and V_h is the hydrodynamic volume. van der Waals volumes of DGLs were calculated on the basis of atomic increments[36] using the following equation:

$$V_W(\text{nm}^3) = 0.1226 \times N + 0.0186 \tag{18}$$

where N is the degree of polymerization.

As shown in Table 4, the free volume fraction also passes through a maximum for the fourth generation. It is also worth noting that DGLs have relatively high free volume fractions that allow the insertion of small molecules in the core of the dendritic structure.

5. Conclusion

TDA was found to be the most appropriate technique for determining the R_h of DGLs. The contribution of the aggregates to the overall signal is much lower in TDA than in DLS or SEC coupled to light scattering detection. Indeed, in TDA, the UV signal is proportional to the mass concentration of the solutes, whatever their hydrodynamic radius, while the scattering intensity scales with R^6. As a consequence, the average hydrodynamic value obtained by TDA ($\langle R_h \rangle_{TDA}$) corresponds to the weight average hydrodynamic value ($\langle R_h \rangle_W$). TDA is also a simple and absolute method that does not require any calibration. Regarding their physicochemical behavior, DGLs are very similar to trifunctional dendrimers (exponential growth of the molar mass, almost linear variation of the hydrodynamic radius, high branching density, and maximum of the intrinsic viscosity for generation 4), except that the molar masses increase more rapidly with generations and that polydispersities are higher than for true dendrimers. The physicochemical characteristics obtained in this work confirm that the polymerization of NCA in buffered water (carbonate buffer at pH 6.5) can lead to DGLs with relatively low polydispersities (<1.5).

Acknowledgment. Sandrine Olivier from Viscotek Europe is gratefully acknowledged for the SEC-triple detection experiments and for stimulating discussions. Sandrine Vieules from Malvern Instruments is gratefully acknowledged for the loan of the Zetasizer Nano ZS apparatus. We thank Manuel Bazzana, Julie Gatinois, and Négar Mesbahi for their contribution to the DLS measurements.

Appendix

Corrections of the Two First Moments of the Elution Profile for the Finite Sample Volume. Plate height expressions given by eqs 1 or 5 assume that an infinitely narrow sample is injected at time 0 at the inlet of the capillary. Let $m_{1,corr}$ and $m_{2,corr}$ be the first moment and second central moment of the hypothetical elution profile that would be obtained for such an infinitely narrow sample. These moments are given as

$$m_{1,\text{corr}} = \frac{l_d}{u} \tag{A-1}$$

$$m_{2,\text{corr}} = \frac{Hl_d}{u^2} \tag{A-2}$$

where l_d is the distance from the capillary inlet to the detector, and u is the cross-sectional averaged flow velocity. In practice, at the origin of time, when the mobilizing pressure is applied, a finite volume, V_i, of sample has been injected in the capillary, occupying a length L_i within the capillary. The mean elution time, m_1, is the time required for the center of the sample zone (which, at time 0, is at distance $L_i/2$ from the capillary inlet) to move up the detector:

$$m_1 = \frac{l_d - \frac{L_i}{2}}{u} \quad \text{(A-3)}$$

The variance of the elution profile is the sum of the variance of an infinitely narrow zone migrating over a distance $l_d - L_i$ and of the temporal variance of the distribution of arrival times to the initial position at distance L_i from the capillary inlet. Assuming that the latter corresponds to that of a uniformly distributed zone of length L_i displaced at velocity u, one gets

$$m_2 = \frac{1}{u^2}\left[H(l_d - L_i) + \frac{L_i^2}{12}\right] \quad \text{(A-4)}$$

Combining eqs A-1 and A-3, and noting that L_i/l_d is equal to V_i/V_c, where V_c is the volume of the capillary from the inlet to the detector, i.e., $\pi d_c^2 l_d/4$, one obtains eq 11. Then, combining eqs A-1, A-2, A-4, and 11, one obtains eq 12.

References and Notes

(1) Schachman, H. K. In *Methods in Enzymology*; Colowick, S. P., Kaplan, N. O., Eds.; Academic Press: New York, 1957; Vol. 4.
(2) Van Holde, K. E.; Baldwin, R. L. *J. Phys. Chem.* **1958**, *62*, 734−743.
(3) Berne, B. J.; Pecora, R. In *Dynamic Light Scattering*; Wiley-Interscience: New York, 1976.
(4) Stejskal, E. O.; Tanner, J. E. *J. Chem. Phys.* **1965**, *42*, 288−292.
(5) Bos, J.; Tijssen, R. In *Chromatography in the Petroleum Industry* (*J. Chrom. Library*, Vol. 56); Adlard, E. R., Ed.; Elsevier: Amsterdam, 1995.
(6) van Asten, A. C.; van Dam, R. J.; Kok, W. Th.; Tijssen, R.; Poppe, H. *J. Chromatogr. A* **1995**, *703*, 245−263.
(7) Walbroehl, Y.; Jorgenson, J. W. *J. Microcolumn Sep.* **1989**, *1*, 41−45.
(8) Yao, Y. J.; Li, S. F. Y. *J. Chromatogr. Sci.* **1994**, *32*, 117−120.
(9) Stellwagen, E.; Stellwagen, N. C. *Electrophoresis* **2002**, *23*, 2794−2803.
(10) Taylor, G. *Proc. R. Soc. London, Ser. A* **1953**, *219*, 186−203.
(11) Aris, R. *Proc. R. Soc. London, Ser. A* **1956**, *235*, 67−77.
(12) Grushka, E.; Kikta, E. J. *J. Phys. Chem.* **1974**, *78*, 2297−2301.
(13) Bello, M. S.; Rezzonico, R.; Righetti, P. G. *Science* **1994**, *266*, 773−776.
(14) Boyle, W. A.; Buchholz, R. F.; Neal, J. A.; McCarthy, J. L. *J. Appl. Polym. Sci.* **1991**, *42*, 1969−1977.
(15) Mes, E. P. C.; Kok, W. Th.; Poppe, H.; Tijssen, R. *J. Polym Sci., Part B: Polym. Phys.* **1999**, *37*, 593−603.
(16) Tomalia, D. A.; Fréchet, J. M. J. In *Dendrimers and Other Dendritic Polymers*; Fréchet, J. M. J., Tomalia, D. A., Eds.; Wiley Series in Polymer Science; John Wiley and Sons: West Sussex, U.K., 2001.
(17) Tomalia, D. A. *Aldrichim. Acta* **2004**, *37*, 38−57.
(18) Caminade, A.-M.; Majoral, J. P. *Acc. Chem. Res.* **2004**, *37*, 341−348.
(19) Dykes, G. M. *J. Chem. Technol. Biotechnol.* **2001**, *76*, 903−918.
(20) Jeong, M.; Mackay, M. E. *Macromolecules* **2001**, *34*, 4927−4936.
(21) Trande, B. M.; Wagner, N. J.; Mackay, M. E.; Hawker, C. J.; Jeong, M. *Macromolecules* **2001**, *34*, 8580−8585.
(22) Zhou, L. L.; Roovers, J. *Macromolecules* **1993**, *26*, 963−968.
(23) Leclaire, J.; Coppel, Y.; Caminade, A.-M. *J. Am. Chem. Soc.* **2004**, *126*, 2304−2305.
(24) Fritzinger, B.; Scheler, U. *Macromol. Chem. Phys.* **2005**, *206*, 1288−1291.
(25) Kee, R. A.; Gauthier, M.; Tomalia, D. A. In *Dendrimers and Other Dendritic Polymers*; Fréchet, J. M. J., Tomalia, D. A., Eds.; Wiley Series in Polymer Science; John Wiley and Sons: West Sussex, U.K., 2001.
(26) Klok, H.-A.; Rodriguez-Hernandez, J. *Macromolecules* **2002**, *35*, 8718−8723.
(27) Klok, H.-A.; Gatti, M.; Rodriguez-Hernandez, J. *Biomacromolecules* **2003**, *4*, 249−258.
(28) Souaïd, E. Ph.D. Thesis, Université de Montpellier 2, 2005.
(29) Yamaguchi, T.; Adachi, K. *Biochem. Biophys. Res. Commun.* **2002**, *290*, 1382−1387.
(30) Sharma, U.; Gleason, N. J.; Carbeck, J. D. *Anal. Chem.* **2005**, *77*, 806−813.
(31) Mourey, T. H.; Turner, S. R.; Rubenstein, M.; Frechet, J. M.; Hawker, C. J.; Wooley, K. L. *Macromolecules* **1992**, *25*, 2401−2406.
(32) Pusey, P. N.; van Megen, W. *J. Chem. Phys.* **1984**, *80* (8), 3513−3520.
(33) Cottet, H.; Biron, J.-P.; Martin, M. *Anal. Chem.*, in revision, 2007.
(34) Wong, S.; Appelhans, D.; Voit, B.; Scheler, U. *Macromolecules* **2001**, *34* (67), 678−680.
(35) Scherrenberg, R.; Coussens, B.; van Vliet, P.; Edward, G.; Brackman, J.; Brabander, E. de.; Mortensen, K. *Macromolecules* **1998**, *31*, 456−461.
(36) Edward, J. T. *J. Chem. Educ.* **1970**, *47*, 261−270.
(37) Manning, G. S. *J. Phys. Chem.* **1981**, *85*, 1506−1515.
(38) Cottet, H.; Gareil, P. *Electrophoresis* **2000**, *21*, 1493−1504.
(39) Tricot, M. *Macromolecules* **1983**, *17*, 1698−1704.

BM070268J